Eurasian Chemico-Technological Journal 21 (2019) 3–12

https://doi.org/10.18321/ectj780

Thermal and Structural Stabilities of Li_xCoO_2 Cathode for Li Secondary Battery Studied by a Temperature Programmed Reduction

D.-H. Jung[1], N. Umirov[1], T. Kim[1], Z. Bakenov[2], J.-S. Kim[3], S.-S. Kim[1,2]*

[1]Chungnam National University, 99 Daehak-ro, Yuseong-gu, Daejeon 34134, Republic of Korea
[2]National Laboratory Astana, School of Engineering, Nazarbayev University, 53, Kabanbay Batyr Ave., Astana 010000, Kazakhstan
[3]Samsung SDI, 467 Beonyeong-ro, Seobuk-gu, Cheonan-si, Chungcheongnam-do 331-300, Republic of Korea

Article info

Received:
04 September 2018

Received in revised form:
20 October 2018

Accepted:
25 December 2018

Keywords:
thermal stability,
temperature programmed reduction,
lithium cobalt oxide,
secondary battery.

Abstract

Temperature programmed reduction (TPR) method was introduced to analyze the structural change and thermal stability of Li_xCoO_2 (LCO) cathode material. The reduction peaks of delithiated LCO clearly represented the different phases of LCO. The reduction peak at a temperature below 250 °C can be attributed to the transformation of CoO_2–like to Co_3O_4–like phase which is similar reduction patterns of CoO_2 phase resulting from delithiation of LCO structure. The 2nd reduction peak at 300~375 °C corresponds to the reduction of Co_3O_4–like phase to CoO–like phase. TPR results indicate the thermal instability of delithiated LCO driven by CoO_2–like phase on the surface of the delithiated LCO. In the TPR kinetics, the activation energies (E_a) obtained for as-synthesized LCO were 105.6 and 82.7 kJ mol^{-1} for T_{m_H1} and T_{m_H2}, respectively, whereas E_a for the delithiated LCO were 93.2, 124.1 and 216.3 kJ mol^{-1} for T_{m_L1}, T_{m_L2} and T_{m_L3}, respectively. As a result, the TPR method enables to identify the structural changes and thermal stability of each phase and effectively characterize the distinctive thermal behavior between as-synthesized and delithiated LCO.

1. Introduction

Lithium-ion batteries (LIB) have been used in various fields from mobile devices to automobiles/energy storage devices due to numerous advantages such as light in weight, high energy density, high power density and long cycle life [1–7]. However, the battery safety is an essential issue to overcome, as the battery are required higher power density and larger capacity.

Many efforts have been conducted to improve the safety of LIB in the active material processing, as well as the cell battery manufacturing and management technology [7–12]. Especially, the thermal stability of LCO has been intensively investigated compared with those of other cathode materials to predict the thermal behaviors of lithium-ion cell. Various methods were introduced to investigate the thermal behaviors. Generally, the decomposition of LCO was measured using the weight loss with the increase of temperature by thermogravimetry (TG). Moreover, their gases evolved were analyzed in-situ by thermogravimetry-mass spectrometry (TG-MS). Dahn et al. proposed the reaction mechanism of LCO decomposition from the weight loss and the O_2 evolution of $Li_{0.4}CoO_2$ at 220 °C, which occurred as the following equation [1, 7].

$$Li_xCoO_2 \rightarrow x\ LiCoO_2 + (1\text{-}x)/3\ Co_3O_4 + (1\text{-}x)/3\ O_2 \quad (1)$$

The exothermic behavior of LCO was also measured by differential scanning calorimetry (DSC). Using the DSC study, Baba et al. reported that the decomposition temperature of LCO in the presence of an electrolyte (~200 °C) was lower than that of chemically delithiated LCO (230 °C) due to solvent decomposition on the LCO surface. This phenomenon is explained by the reducing power of the solvent, which is identified by oxidation of electrolyte solvent [7]. The research on the self-heating characteristics of LCO active material was also studied by accelerating rate calorimetry (ARC).

*Corresponding author. E-mail: kimss@cnu.ac.kr

Although these methods provide very useful information on the thermal behavior and safety of the LCO, it is difficult to explain the nature of LCO alone. Since the information is resulted from complex electrochemical reactions influenced by various factors, including electrode consisting materials such as conducting agents, binders, electrolyte solvents and salts, as well as their composition in the battery cell. To obtain the decomposition of LCO itself without other reactions involved, Furushima et al. quantified the O_2 evolution rate with chemically delithiated LCO ($Li_{0.65}CoO_2$ and $Li_{0.81}CoO_2$) by using a temperature programmed desorption-mass spectrometry (TPD-MS) and determined the activation energy of the delithiated LCO decomposition kinetics [11]. Yamaki et al. also studied on the O_2 evolution from delithiated LCO state [12]. The onset temperature of O_2 evolution by TG-MS was shifted from 240 °C to 210 °C with micro-sized (1~5 mm) and nano-sized (200~400 nm) materials, respectively. The difference between micro- and nano-sized LCO active material was explained by the surface area due to the particle size, and the frequency factor was optimized for the nano-sized LCO. Furthermore, the chemical states of overcharged LCO surfaces and interiors were observed in the recent literature [13, 14]. They reported that LCO, delithiated by overcharging, has Co_3O_4–like and CoO_2–like phases at the surface region and lithium-rich LCO phases at the core region showing a gradient of lithium contents between the surface and the core of the delithiated LCO. They explained that the key factors affecting the degradation are nano-cracks with deficient Li-ions on the surface of LCO.

Therefore, in this study, we investigated the characteristics of LCO by a thermochemical reaction using a simple temperature programmed reduction (TPR) with H_2 (reducing reagent). The thermal behavior and phase changes of LCO were examined without the electrochemical charge-discharge and those of LCO compared with the delithiated LCO (charged state) after the electrochemical activation. In addition, kinetic studies were conducted to quantify the thermal stability of as-synthesized LCO and delithiated LCO in each phase in the TPR.

2. Experimental

The synthesized of LCO powder was prepared by a solid-state mixing of Li_2CO_3 (Umicore) and Co_3O_4 (Junsei Chemical) and calcined at 875 °C for 8 h in air flow. The heat-treatment of LCO was performed at 450 °C for 3 h. The calcined sample was crushed to 1~5 μm using ball milling and sieving.

X-ray diffractometer (Rint-2000, Rigaku) was used to identify the crystallinity of as-synthesized LCO and delithiated Li_xCoO_2 state using CuKá X-ray radiation. The spectra were scanned with a step size of 0.03° in the range of 10~90°.

The cathode electrode was fabricated through a mixing, coating, drying and pressing process. The composition of the electrode was 96 wt% active material ($LiCoO_2$), 2 wt% conducting agent (SuperP, TIMCAL) and 2 wt% polyvinylidene fluoride (PVDF, Solef) binder. A homogenous slurry mixture was made by a homogenizing mixer (2000 rpm, ARE-310, Thinky) with the electrode components in N-methyl-2-pyrrolidone (NMP) solvent and the slurry was coated on aluminum foil to be loaded 10 mg cm^{-2} of $LiCoO_2$. The coated electrode was dried at 120 °C for 0.5 h and pressed to be the electrode density of 3.6 g cm^{-3}.

For all electrochemical tests and spectroscopic analyses, coin cells (2016 type) were assembled in an argon-filled glove box. The cells consisted of a positive electrode, Li metal as a negative electrode, a microporous separator (Celgard 2500) and an electrolyte of ethylene carbonate (EC), ethyl methyl carbonate (EMC) and dimethyl carbonate (DMC) (1:1:1 volume ratio, Panax E-Tec Co.) with a 1M $LiPF_6$ salt. The electrochemical performances were tested in the galvanostatic mode using a battery cycler (Won A tech, WBCS 3000) in the voltage range of 3.0 and 4.3 V. For delithiated LCO, the coin cells were electrochemically activated with the same steps through an aging for 1 day, the activation with 1st charge-discharge, the capacity measurement of 2nd charge-discharge and the final charge up to a desired voltage to adjust the state of charge (SOC) or lithium contents of LCO [14].

The thermal stability of LCO materials were investigated by DSC (Mettler Toledo). For the DSC analysis, delithiated LCO which was electrochemically fully charged up to 4.3 V was taken from coin cells in an argon-filled glove box. The sample was loaded in a stainless steel high pressure pan and measured with a heating rate of 5 °C min^{-1}. The reduction behaviors of as-synthesized LCO and delithiated LCO were analyzed by TPR with H_2. The reference materials, including quartz wool, Li_2O, LiOH, Li_2CO_3 and Co_3O_4, were also measured under the same conditions. The TPR was carried out in a quartz tubular reactor equipped with a thermal conductivity detector (TCD).

TCD was used to determine the amount of H_2 consumption. 10 mg of the sample was loaded in the reactor and 4% H_2/Ar was fed at a rate of 10 ml min^{-1}. The reduction of cathode material was observed in the temperature range of 100 to 760 °C at different heating rates of 2, 5, 10 °C min^{-1} [15–18]. For TPR analysis, electrochemically delithiated LCO was taken from the coin cell and the electrode disk was cleaned with dimethyl carbonate solvent and dried in an argon-filled glove box.

3. Results and discussion

3.1. Electrochemical performance

The electrochemical performances of synthesized LCO are shown in Fig. 1. The initial 3 cycles were measured at a 0.1C charge/discharge rate and from the 4^{th}~50^{th} cycles were measured at a 0.5C charge/discharge rate. The initial discharge capacity was 158 mAh g^{-1} (0.1C charge – 0.1C discharge) with coulombic efficiency of 95.6%, and the discharge capacity after 50 cycles (0.5C charge – 0.5C discharge) was 87.4% of the initial one. The specific capacity of LCO appears a typical behavior in the charge (4.3 V) and discharge (3.0 V) process compared with previous studies [2, 5]. The cycle life indicates good stability with high capacity retention in the half coin cell. In the charge-discharge profile after 50 cycles, an increase of charge voltage and a decrease of discharge voltage were observed, which attributed to the current increase according to the C-rate increase from 0.1 to 0.5 as well as the deterioration of LCO in the progress of the cycle.

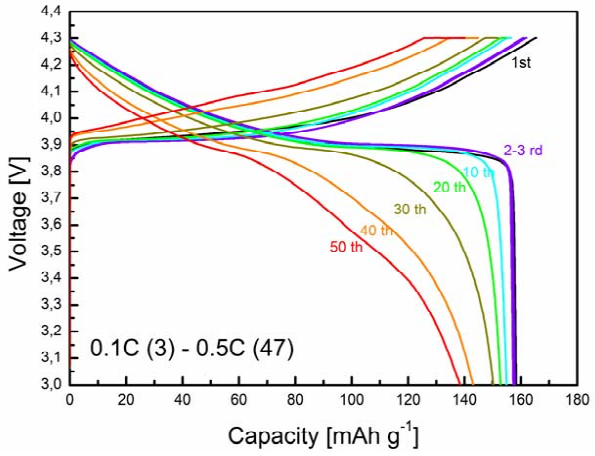

Fig. 1. Electrochemical performance of as-synthesized LCO. The 1^{st}~3^{rd} charge/discharge profiles were measured at 0.1C rate and 4^{th}~50^{th} profiles were measured at 0.5C rate.

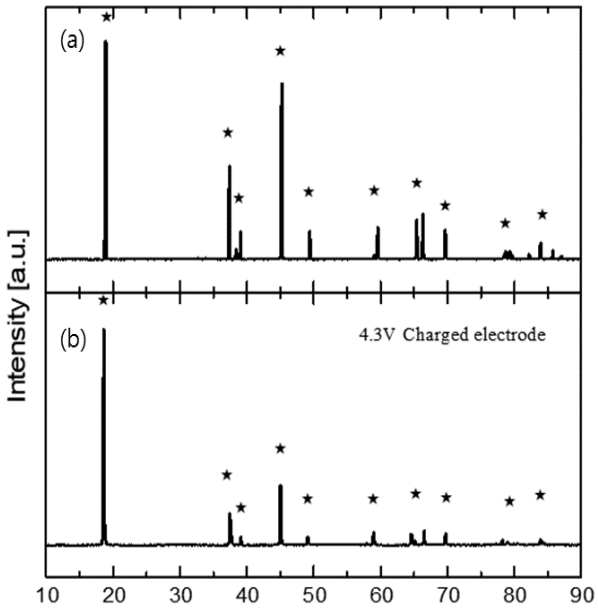

Fig. 2. XRD patterns of (a) as-synthesized LCO and (b) delithiated LCO (4.3 V charged).

Figure 2 shows XRD patterns of as-synthesized LCO and delithiated LCO (4.3 V charged state). As-synthesized LCO shows a strong (003) diffraction peak, slightly strong other (00l) peaks and other relatively weak peaks. When the LCO was charged up to 4.3 V, the (003) peak decreases to a lower angle from 18.9 to 18.6 resulted from the layered structure expansion. In the previous study [6], however, the (003) peak increases with charged state above 4.5 V which was explained by a contraction of the host structure along the c-axis due to the decrease of charged oxygen ions followed by lowered electrostatic repulsion between the oxygen ions.

3.2. Thermal behavior in DSC

The thermal behaviors of as-synthesized LCO and delithiated LCO (4.3 V charged) in the presence of the electrolyte (EC/EMC/DMC=1/1/1 with 1M $LiPF_6$ salt), by DSC analysis are shown in Fig. 3. The electrolyte used in the experiment showed exothermic behaviors which have a peak temperature around 250 °C and a broad area of the peak (Fig. 3(a)). In the case of as-synthesized LCO with the electrolyte (Fig. 3(b)), the exothermic peak area is significantly smaller than that of the electrolyte itself. No exothermic peaks are observed with as-synthesized LCO alone under 400 °C (not shown in Fig. 3), therefore, the reduced area of the exothermic peak can be attributed to the relatively small amount of the electrolyte in the sample rather

than mixed behavior between LCO and the electrolyte. The calorific values are obtained as 431.7 J g^{-1} and 106.6 J g^{-1} for the electrolyte only and as-synthesized LCO with electrolyte, respectively. In the as-synthesized LCO with electrolyte, the amount of heat generation (1st peak) is lower than that of the expected calorific value (141.9 J g^{-1}) calculated from the equivalent amount of electrolyte, however, sample b shows 2nd exothermic peak at higher temperature ~290 °C which has 100.5 J g^{-1} due to the reaction between LCO and the electrolyte. The delithiated LCO with electrolyte (Fig. 3(c)) shows two major exothermic peaks at lower temperature (~220 °C) with relatively high calorific value of 543.0 J g^{-1}. Yamaki et al., in their TG-MS and DSC studies with $Li_{0.49}CoO_2$, reported that 1st peak at ~200 °C should be attributed to a surface reaction of $Li_{0.49}CoO_2$ with the electrolyte without O_2 evolution and 2nd peak at higher temperature is likely to be caused by oxidation of the electrolyte by the O_2 evolution [10].

From DSC analysis, the thermal parameters such as the on-set and maximum temperature and the calorific value of the exothermic reactions have been obtained [8–10, 12, 19]. However, the results of as-synthesized LCO and delithiated LCO cannot be represent the active materials' characteristics since they are not only resulted from LCO itself but the reactions of LCO with the electrolyte, conducting material and the binder. Thus, two peaks observed in the delithiated LCO cannot explain clearly each reaction step with the separation of the two phases.

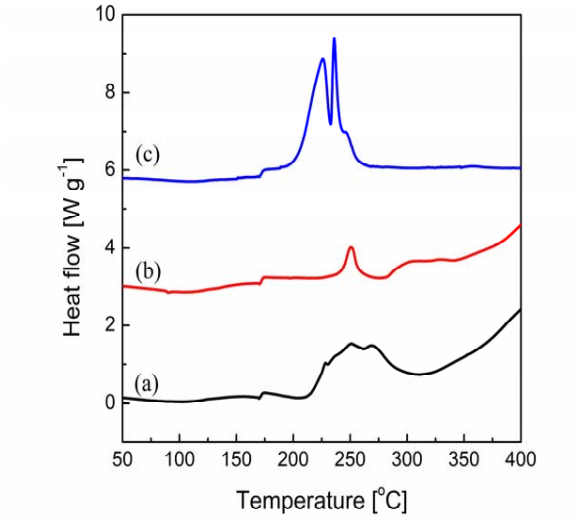

Fig. 3. DSC thermograms for (a) electrolyte 2 mg (1M $LiPF_6$ in EC/EMC/DMC=1/1/1) (b) as-synthesized LCO 1.5 mg and electrolyte 0.75 mg and (c) delithiated LCO (4.3 V charged) 1.5 mg and electrolyte 0.75 mg.

3.3. Thermal behavior and reduction mechanism in TPR

To investigate clear degradation reaction mechanism of LCO, TPR characterization is employed as a complementary method which is expected to provide a structural stability of the metal oxide active material in the reduction conditions with the increase of temperature.

As shown in Fig. 4, the baseline of an empty tubular reactor with a quartz wool as a sample supporter ((Fig. 4(a)) is stable without H_2 consumption up to 650 °C. For LiOH (Fig. 4(c)) and Li_2CO_3 (Fig. 4(d)) as Li sources of LCO synthesis, LiOH is very stable below 400 °C, but H_2 outgassing is observed at 450 °C. Similar reactions from $LiH/Li_2O/LiOH$ system on H_2 outgassing were reported as below [20].

$$LiOH + H_2 \rightarrow LiH + H_2O \quad (2)$$

$$LiOH + LiH \rightarrow Li_2O + H_2 \quad (3)$$

Generally, Li_2CO_3 is thermally decomposed without H_2 reduction at high temperature in the range of 730–1270 °C [21]. In the TPR experimental temperature range (<650 °C), Li_2CO_3 shows a stable behavior (Fig. 4(d)).

$$Li_2CO_3 \rightarrow Li_2O + CO_2 \quad (4)$$

However, in the case of metal oxide, Co_3O_4 is reduced via typical two step reaction mechanisms ($Co_3O_4 \rightarrow CoO \rightarrow Co$) [16, 17]. Two peaks according to the two step reaction are observed in the TPR analysis for Co_3O_4 (Fig. 4(e)).

$$CO_3O_4 + H_2 \rightarrow 3CoO + H_2O \quad (5)$$

$$CoO + H_2 \rightarrow 3Co + H_2O \quad (6)$$

As-synthesized LCO is reduced at a higher temperature compared to those of Co_3O_4, and shows a similar two-step reduction (Fig. 4(f)). A possible mechanism of LCO reduction is the reaction of Eqs. (7) and (6).

$$2LiCoO_2 + H_2 \rightarrow Li_2O + 2CoO + H_2O \quad (7)$$

Li_2O decomposed from LCO reduction can be reacted with H_2O and has an equilibrium with LiOH compound as below Eq. (8) [22]. The Li_2O shows relatively stable behavior compared with that of LiOH in TPR analysis (Fig. 4(b)).

$$Li_2O + H_2O \rightarrow 2LiOH \quad (8)$$

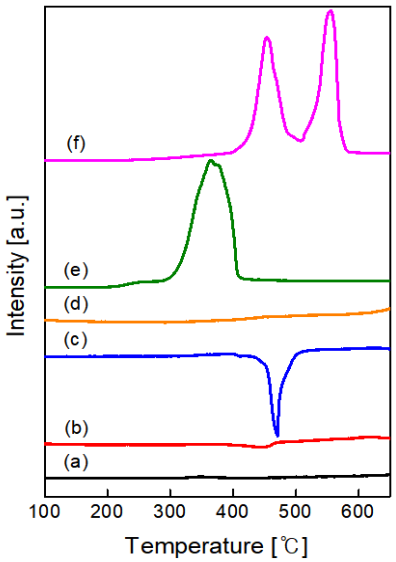

Fig. 4. TPR profiles of as-synthesized LCO and raw materials, (a) quartz wool, (b) Li_2O, (c) LiOH, (d) Li_2CO_3, (e) Co_3O_4, and (f) as-synthesized LCO with heating rate of 5 °C min^{-1}.

Above TPR results of as-synthesized LCO show clear structural change with the increase of temperature unlike DSC thermograms. Thus, it is considered that TPR analysis can be applied as a suitable method to investigate the thermal behavior and related structural change of metal oxide active materials. Moreover, TPR method can simply analyze the thermal behavior of LCO itself without an effect of the electrolyte.

Based on the TPR results of as-synthesized LCO and the raw materials, TPR patterns of LCO with the increase of delithiation state were investigated as shown in Fig. 5. The delithiation state was represented by the ratio of the charge capacity to the theoretical capacity of 274 mAh g^{-1} when $x = 1$ in Li_xCoO_2. The SOC denotes the percentage ratio (%) of the charge capacity on the basis of the one of LCO up to 4.3 V with 158 mAh g^{-1}. As-synthesized LCO sample shows much higher reduction temperatures than those of delithiated LCO. This can be attributed to the strong layered structure, which composed at high temperature (870 °C). As-synthesized LCO shows two reduction peaks appeared at high temperature above 400 °C in the TPR profile. The 1st peak mainly corresponds to the reduction of Co^{3+} and Co^{4+} to Co^{2+}, and the 2nd peak to the reduction of Co^{2+} to Co^0 [23]. However, in the case of delithiated LCO, the reduction peaks are observed at a much lower temperature. The reduction peaks at low temperatures below 250 °C may be attributed to the transformation of CoO_2–like to Co_3O_4–like phase, which appears similar reduction patterns of CoO_2 phase resulting from the delithiation of LCO structure and the 2nd reduction peak at 300~375 °C corresponds to the reduction of Co_3O_4–like phase to CoO–like phase.

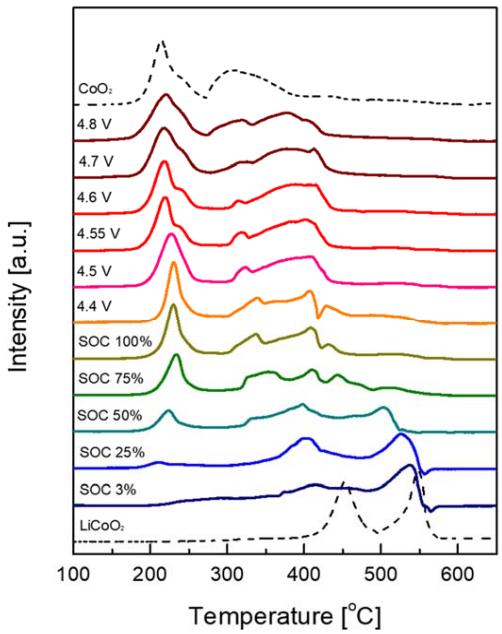

Fig. 5. TPR patterns of Li_xCoO_2 with the increase of delithiation state (5 °C min^{-1} heating rate).

LCO of $x = 0.98$ state (SOC 3%) after the electrochemical charge and discharge shows a broad and weak reduction peak in the temperature range of 200~350 °C and relatively strong two peaks at 410 and 540 °C which are lower temperatures compared with those of as-synthesized LCO ($x = 1$). The former may be attributed to the lithium loss due to the irreversible contents (~2.6%) of the initial charge and discharge process and the latter may be referred to the existence of a considerable amount of lithium-deficient phase on the surface of LCO and the residual by-product of the electrolyte on the surface of LCO in spite of DMC washing.

Two-step reduction peaks of as-synthesized LCO are observed with the increase of SOC 50% ($x = 0.71$) although the intensity of peaks are reduced and shifted to a lower temperature. However, TPR pattern of the SOC 75% ($x = 0.56$) state revealed drastic change with the occurrence of the strong reduction peak around 220 °C and the disappearance of 2nd peak in the two-step reduction of as-synthesized LCO above 500 °C. These changes of TPR can be comparable to the structural phase transitions of LCO charge-discharge curves [6] corresponding to the metal-insulator transition around 3.9 V charged ($x = \sim 0.7$) and the order-disorder transitions between 4.05 V and 4.20 V charged ($x = \sim 0.5$).

The intensity of reduction peak at 220 °C increases with the increase of the delithiation state in the range from x = 0.42 (4.3 V charged) to x = 0.36 (4.4 V charged). As the delithiation further progresses to the state of x = 0.29 (4.5 V charged), the main peak becomes broader and the on-set temperature decreases to the temperature lower than 200 °C. The result indicates that the thermal stability of LCO is deteriorated significantly as increase of the delithiation in the LCO structure.

On the other hand, the reduction peak of x = 0.2 (4.55 V charged) shows a clear phase change with the separated reduction peak at 200 °C. Also, at a charge of 4.7 V or more (x = 0.15), the peak at 200 °C was observed as a main peak and the peak at 220 °C was diminished gradually. The result corresponds to the transition from the O3 phase to H1-3 phase and from the H1-3 phase to O1 phase in the results of dQ/dV curve which have two transition peaks at 4.55 V and 4.62 V [6].

In order to elucidate the phase at 200 °C, a fully delithiated CoO_2 phase was prepared by charge up to 5.0 V (3 days continuous charge) and the reduction temperature of CoO_2 phase is in good agreement with the transition peak at 200 °C. The CoO_2 phase has been investigated for its existence as an end member of LCO [2, 3]. The results of the TPR, also, exactly matched in the previous differential thermogravimetry (DTG) with 5% H_2/Ar gas flow study reported by Motohashi et al. [24] and they proposed two step reductive reactions of CoO_2-δ → CoO → Co. They explained that it is in the equilibrium under unstable state of oxygen deficiency with the (2-δ) value in the range of 1.72 to 1.92. The oxygen content (2-δ) of CoO_2 depends strongly on the synthesis procedure such that the more equilibrated synthesis and/or more highly oxidizing conditions tend to suppress the formation of oxygen vacancies.

In a view of thermal stability, the exothermic behavior of LCO occurs below 200 °C which depends on the reaction between LCO and the electrolyte in the case of DSC analysis, whereas the reduction of LCO itself starts at 200 °C with all the variation of SOC and overcharge level except x = 1 in the case of TPR analysis. TPR results indicate the thermal instability of delithiated LCO driven by CoO_2–like phase on the surface of the delithiated LCO. Ohzuku et al. observed a stability of monoclinic phase (x = 0.55, OCV 4.12) with XRD study, which examine the average bulk structure regardless of surface variations [2].

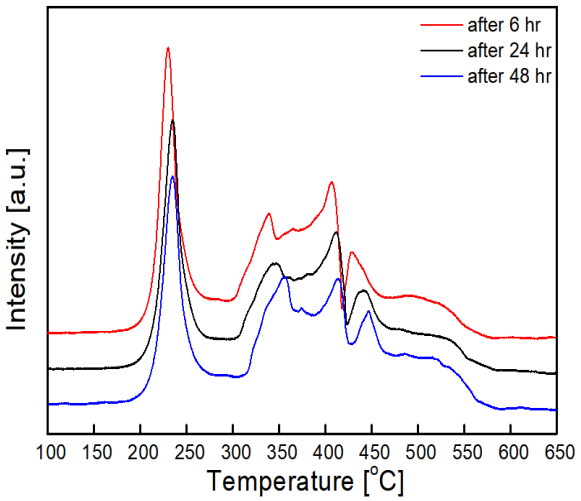

Fig. 6. TPR patterns for delithiated LCO (4.3 V charged) with different aging times at room temperature.

In this TPR study, Fig. 6 shows TPR patterns of delithiated LCO with different aging time at room temperature. Peak temperature of CoO_2–like phases at around 220 °C is shifted during an initial aging of 24 h, whereas, the peak temperature of Co_3O_4–like phases at around 340 °C is shifted sequentially after 24 h. This time lag between the peak shifts can be explained that CoO_2–like phases on the surface of Li_xCoO_2 are quickly stabilized through contacting Li ions polarized in electrolyte, whereas Co_3O_4–like phases in the core of Li_xCoO_2 are much slowly changed via Li ion diffusion in the solid state. This implies that TPR method can resolve surface and core effect.

3.4. TPR kinetics of as-synthesized LCO and delithiated LCO

TPR spectra has been analyzed not only qualitatively to compare materials but also to estimate the respective kinetic parameter as well [25]. For the TPR kinetics of as-synthesized LCO and delithiated LCO solid state materials, the Kissinger Method [26, 27] was applied, since it is a simple approach to determine the activation energies under the condition of the maximum reaction rate. In general, the rate of the non-isothermal TPR can be described as follows:

$$\frac{d\alpha}{dt} = \left(\beta \frac{d\alpha}{dT}\right) = k(T) f(\alpha) \qquad (9)$$

where t, α and β represent the time, the rate of conversion and a constant heating rate in a function of

the reaction model $f(\alpha)$ and the temperature dependence of rate constant, $k(T)$ which is expressed by the Arrhenius equation.

$$\frac{d\alpha}{dt} = \left(\beta \frac{d\alpha}{dT}\right) = k(T) f(\alpha) \qquad (10)$$

where A, E, T and R are the pre-exponential factor, the activation energy (J mol^{-1}), the reaction temperature and the gas constant (8.314 J mol^{-1} K^{-1}). By using the above equations, the reaction rate can be expressed as:

$$-\frac{E_a \beta}{RT_m^2} = Af'(\alpha_m) exp\left(\frac{-E_\alpha}{RT_m}\right) \qquad (11)$$

where $f'(\alpha) = df(\alpha)/d\alpha$ and the subscript m denotes the value of maximum. From the logarithm rearrangements, Kissinger equation (Eq. (12)) obtained under the assumption of the reaction is the first order and the independent of heating rate.

$$\ln\left(\frac{\beta}{T_m^2}\right) = \ln\left(-\frac{AR}{E}\right) - \frac{E}{RT_m} \qquad (12)$$

The maximum reduction temperatures are obtained with different heating rates as shown in Fig. 7. TPR patterns of as-synthesized LCO and delithiated LCO (4.3 V charged state) with different heating rates (2, 5, 10 °C min^{-1}). As-synthesized LCO shows two reduction peaks in the TPR profile. The 1st peaks mainly correspond to the reduction of Co^{3+} and Co^{4+} to Co^{2+}. They are appeared at high temperature above 400 °C with different heating rates (T_{m_H1} 421.4, 452.5 and 481.3 °C for 2, 5 and 10 °C min^{-1} heating rate). The 2nd peaks correspond to the reduction of Co^{2+} to Co^0. The temperatures of 2nd peaks (T_{m_H2}) with different heating rates are 502.6, 548.2 and 596.9 °C for heating rate of 2, 5 and 10 °C min^{-1}, respectively. However, in the case of delithiated LCO, the reduction peaks are observed at a much lower temperatures. The 1st reduction peaks at low temperatures below 250 °C (212.2, 230.3 and 245.5 °C for 2, 5 and 10 °C min^{-1} heating rate) may be attributed to the transformation of (i) CoO_2–like to Co_3O_4–like phase, which appears similar reduction patterns of CoO_2 phase resulting from the delithiation of LCO structure. The 2nd reduction peaks (325.3, 340.5 and 362.7 °C for 2, 5 and 10 °C min^{-1} heating rate) correspond

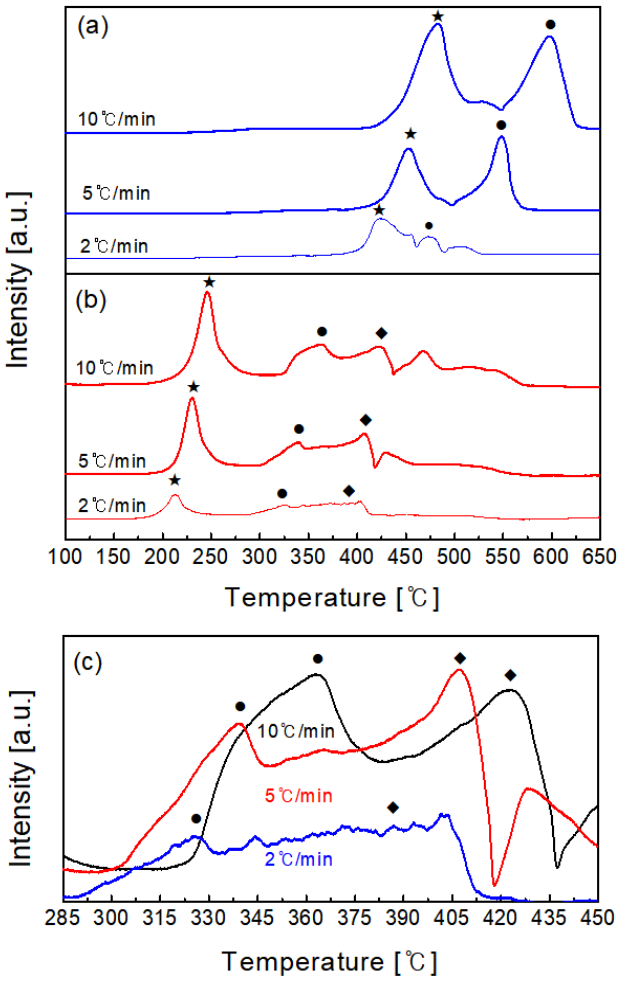

Fig. 7. TPR patterns of (a) as-synthesized LCO, (b) delithiated LCO (4.3 V charged state) and (c) magnified graph of delithiated LCO (4.3 V charged state) with different heating rates.

to the reduction of (ii) Co_3O_4–like phase to CoO–like phase. Finally, the 3rd reduction peaks at 386.9, 407.4 and 423.4 °C for 2, 5 and 10 °C min^{-1} heating rate, correspond to the reduction of (iii) CoO–like phase to Co^0.

From the above the maximum temperature (T_m) of the TPR experiment with different heating rates, kinetic parameters for as-synthesized LCO and delithiated LCO (4.3 V charged) are obtained by Kissinger method as shown in Fig 8. The E_a obtained for the as-synthesized LCO was 105.6 and 82.7 kJ mol^{-1} for T_{m_H1} and T_{m_H2}, respectively. This indicates that the first reduction (1st peak) of as-synthesized LCO requires high temperature (421.4~481.3 °C) and relatively large activation energy due to the highly crystallized layer-structure, then the second reduction (2nd peak) requires relatively small activation energy once the structure collapsed at the first reduction.

Whereas, E_a for delithiated LCO was 93.2 and 124.1 and 216.3 kJ mol^{-1} for T_{m_L1}, T_{m_L2} and T_{m_L3}, respectively. This represents the reduction of delithiated LCO requires low temperature (212.2~245.5 °C) and relatively small activation energy with high pre-exponential factor compared with as-synthesized LCO. Generally, the activation energy of the CoO_2 reduction reaction decreases as the reduction proceeds as the result of Ji et al. In this study, however, the activation energy increases as the 1st, 2nd and 3rd reduction proceeds since the reaction at the surface, which is the CoO_2-like phase containing a negligible amount of Li ion, occurs at a high rate and then the reaction in the core region which contains more Li ion occurs at a low rate. The kinetic properties are summarized in Table and compared with those of previous studies.

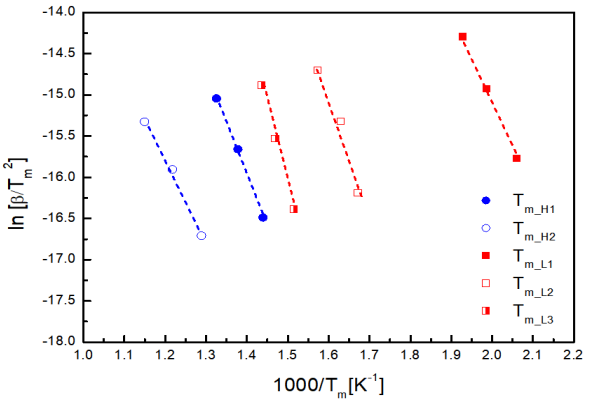

Fig. 8. Kinetics of TPR for the as-synthesized LCO and delithiated LCO (4.3 V charged).

In the previous studies for the kinetics of LCO decomposition, Wang et al. reported that E_a of the Li_xCoO_2 (x = 0.42, 4.2 V charged) was obtained 88.87 kJ mol^{-1} and 148.87 kJ mol^{-1} by DSC (C80) and TG analysis, respectively [9]. They noted that E_a obtained by DSC is smaller than that of TG because E_a from DSC data is calculated near the on-set temperature of Li_xCoO_2 (~170 °C) and kinetics of DSC could result in more reliable, whereas E_a from TG is obtained near the temperature of maximum mass loss (~250 °C). Furushima et al., also, reported kinetic results of the thermal decomposition of chemically delithiated Li_xCoO_2 with the liberated O_2 gas quantified by TPD-MS [11]. They noted that the decrease of Li content in Li_xCoO_2 brings about the lower E_a of thermal decomposition based on the results obtained 130 kJ mol^{-1} for $Li_{0.81}CoO_2$ and 97 kJ mol^{-1} for $Li_{0.65}CoO_2$. On the other hand, Yamaki et al. reported relatively high value of E_a as 114 kJ mol^{-1} for $Li_{0.5}CoO_2$ which is obtained from an average value of activation energies in the range of a = 0.3~0.7 (a is a degree of conversion) assuming two or more reactions as a single reaction [12].

From this TPR kinetic study, it is considered that the 1st reduction reaction of delithiated LCO (CoO_2–like phase) will act as a trigger for thermal runaway and the activation energy is comparable with the one obtained from the DSC on-set temperature among the results of other previous studies.

Table

Summary of kinetic properties reported in the literature and those of present study for the $LiCoO_2$

Authors	Experiment	Material	Temp.	E_a	A	n	R^2
Wang et al. (2008)	TG DSC	$Li_{0.52}CoO_2$ $Li_{0.52}CoO_2$	256 190	148.87 88.87	1.22E+12 1.87E+06	1	0.946 0.998
Furushima et al. (2011)	TPD-MS	$Li_{0.81}CoO_2$ $Li_{0.65}CoO_2$	>250	130 97	- -	1 1	>0.98
Yamaki et al. (2014)	TG-MS	m-$Li_{0.5}CoO_2$ n-$Li_{0.5}CoO_2$	240 210	114	1.88 E+10 3.76 E+10	1.62	<0.99
Ji et al. (2009)	TPR	CoOOH Co_3O_4 CoO	186 248 340	93.1 80 53	- - -	1 1 1	- - -
This study	TPR	$LiCoO_2$ Li-CoO	452.5 548.2	105.6 82.7	2.99E+01 3.62E-01	1 1	0.998 0.993
		$Li_{0.42}CoO_2$ CoO_2-like Co_3O_4-like CoO-like	230.3 340.5 407.4	93.2 123.8 157.5	1.58E+04 9.67E+04 7.27E+06	1 1 1	0.999 0.966 -

4. Conclusions

We investigated the structural change and thermal stability of LCO by a thermochemical reaction using a temperature programmed reduction (TPR) with H_2. As-synthesized LCO has an initial discharge capacity of 158 mAh g^{-1} (4.3 V charged) and shows a stable cycleability, which has 87.4% discharge capacity of the initial one after 50 cycles.

In DSC thermograms, thermal behaviors of as-synthesized LCO shows the reactions with the electrolyte rather than the behaviors of LCO itself and delithiated LCO with electrolyte shows two major exothermic peaks with strong exothermic behaviors at lower temperature (~220 °C). In TPR profile, as-synthesized LCO shows two strong reduction peaks. The 1st peaks mainly correspond to the reduction of Co^{3+}, Co^{4+} to Co^{2+}, and the 2nd peaks correspond to the reduction of Co^{2+} to Co^0. On the other hand, the reduction peaks of delithiated LCO are observed at a much lower temperatures. The reduction peaks at low temperatures below 250 °C may be attributed to the transformation of (i)CoO_2–like to Co_3O_4–like phase, which appears similar reduction patterns of CoO_2 phase resulting from the delithiation of LCO structure. The 2nd reduction peaks at low temperatures (300 and 375 °C), correspond to the reduction of (ii) Co_3O_4–like phase to CoO–like phase. TPR results indicate the thermal instability of delithiated LCO driven by CoO_2–like phase on the surface of the delithiated LCO.

Kinetic parameters for as-synthesized LCO and delithiated LCO (4.3 V charged) are obtained by Kissinger method. The E_a obtained for the as-synthesized LCO were 105.6 and 82.7 kJ mol^{-1} for T_{m_H1} and T_{m_H2}, respectively. Whereas, E_a for delithiated LCO were 93.2 and 124.1 and 216.3 kJ mol^{-1} for T_{m_L1}, T_{m_L2} and T_{m_L3}, respectively.

Acknowledgements

The authors are very grateful for the financial support of the KETEP (Grant 20164010201070) and also thanks to the support from Chungnam National University and the research grant AP05133519 "Development of 3-dimensional thin film silicon based anode materials for next generation lithium-ion microbatteries" from the Ministry of Education and Science of the Republic of Kazakhstan.

References

[1]. J. Dahn, E. Fuller, M. Obrovac, U. Vonsacken, *Solid State Ionics* 69 (1994) 265–270. DOI:10.1016/0167-2738(94)90415-4

[2]. A. Ueda, T. Ohzuku, *J. Electrochem. Soc.* 141 (1994) 2972. DOI: 10.1149/1.2055051

[3]. G. Amatucci, J. Tarascon, L. Klein, *J. Electrochem. Soc.* 143 (1996) 1114–1123. DOI: 10.1149/1.1836594

[4]. M.N. Richard, J.R. Dahn, *J. Electrochem. Soc.* 146 (1999) 2078. DOI: 10.1149/1.1391894

[5]. C. Julien, *Solid State Ionics* 157 (2003) 57–71. DOI: 10.1016/S0167-2738(02)00190-X

[6]. H. Xia, L. Lu, Y.S. Meng, G. Ceder, *J. Electrochem. Soc.* 154 (2007) A337. DOI: 10.1149/1.2509021

[7]. D.D. MacNeil, J.R. Dahn, *J. Electrochem. Soc.* 148 (2001) A1205. DOI: 10.1149/1.1407245

[8]. Z. Zhang, D. Fouchard, J.R. Rea, *J. Power Sources* 70 (1998) 16–20. DOI: 10.1016/S0378-7753(97)02611-6

[9]. Q.S. Wang, J.H. Sun, C.H. Chen, X.M. Zhou, *J. Therm. Anal. Calorim.* 92 (2008) 563–566. DOI: 10.1007/s10973-007-8289-z

[10]. Y. Baba, S. Okada, J. ichi Yamaki, *Solid State Ionics* 148 (2002) 311–316. DOI: 10.1016/S0167-2738(02)00067-X

[11]. Y. Furushima, C. Yanagisawa, T. Nakagawa, Y. Aoki, N. Muraki, *J. Power Sources* 196 (2011) 2260–2263. DOI: 10.1016/j.jpowsour.2010.09.076

[12]. J. Yamaki, Y. Shinjo, T. Doi, S. Okada, *J. Electrochem. Soc.* 161 (2014) A1648–A1654. DOI: 10.1149/2.0621410jes

[13]. J. Kikkawa, S. Terada, A. Gunji, T. Nagai, K. Kurashima, K. Kimoto, *J. Phys. Chem. C.* 119 (2015) 15823–15830. DOI: 10.1021/acs.jpcc.5b02303

[14]. S. Sharifi-Asl, F.A. Soto, A. Nie, Y. Yuan, H. Asayesh-Ardakani, T. Foroozan, V. Yurkiv, B. Song, F. Mashayek, R.F. Klie, K. Amine, J. Lu, P.B. Balbuena, R. Shahbazian-Yassar, *Nano Lett. 1*7 (2017) 2165–2171. DOI: 10.1021/acs.nanolett.6b04502

[15]. A. Nurpeissova, M.H. Choi, J.-S. Kim, S.-T. Myung, S.-S. Kim, Y.-K. Sun, *J. Power Sources* 299 (2015) 425–433. DOI: 10.1016/j.jpowsour.2015.09.016

[16]. C.W. Tang, C. Bin Wang, S.H. Chien, *Thermochim. Acta* 473 (2008) 68–73. DOI: 10.1016/j.tca.2008.04.015

[17]. Y.G. Ji, Z. Zhao, a J. Duan, G.Y. Jiang, J. Liu, *J. Phys. Chem. B.* 113 (2009) 7186–7199. DOI: 10.1021/jp8107057

[18]. J.S. Kim, S. Lee, S.B. Lee, M.J. Choi, K.W. Lee, *Catal. Today* 115 (2006) 228–234. DOI: 10.1016/j.cattod.2006.02.038

[19]. N.S. Choi, I.A. Profatilova, S.S. Kim, E.H. Song, *Thermochim. Acta* 480 (2008) 10–14. DOI: 10.1016/j.tca.2008.09.017

[20]. L.N. Dinh, D.M. Grant, M.A. Schildbach, R.A. Smith, W.J. Siekhaus, B. Balazs, J.H. Leckey, J.R. Kirkpatrick, W. McLean, *J. Nucl. Mater.* 347 (2005) 31–43. DOI: 10.1016/j.jnucmat.2005.06.025

[21]. R. Qiao, Y. De Chuang, S. Yan, W. Yang, *PLoS One* 7 (2012) 3–8. DOI: 10.1371/journal.pone.0049182

[22]. N.W. Gregory, R.H. Mohr, *J. Am. Chem. Soc.* 77 (1955) 2142–2144. DOI: 10.1021/ja01613a030

[23]. E. Markevich, G. Salitra, D. Aurbach, *Electrochem. Commun.* 7 (2005) 1298–1304. DOI: 10.1016/j.elecom.2005.09.010

[24]. T. Motohashi, Y. Katsumata, T. Ono, R. Kanno, M. Karppinen, H. Yamauchi, *Chem. Mater.* 19 (2007) 5063–5066. DOI: 10.1021/cm0702464

[25]. G. Munteanu, L. Ilieva, D. Andreeva, *Thermochim. Acta* 291 (1997) 171–177. DOI: 10.1016/S0040-6031(96)03097-3

[26]. S. Vyazovkin, A.K. Burnham, J.M. Criado, L.A. Pérez-Maqueda, C. Popescu, N. Sbirrazzuoli, *Thermochim. Acta* 520 (2011) 1–19. DOI: 10.1016/j.tca.2011.03.034

[27]. J.S. Kim, W.Y. Lee, S.B. Lee, S.B. Kim, M.J. Choi, *Catal. Today* 87 (2003) 59–68. DOI: 10.1016/j.cattod.2003.10.004